

Supplemental figures

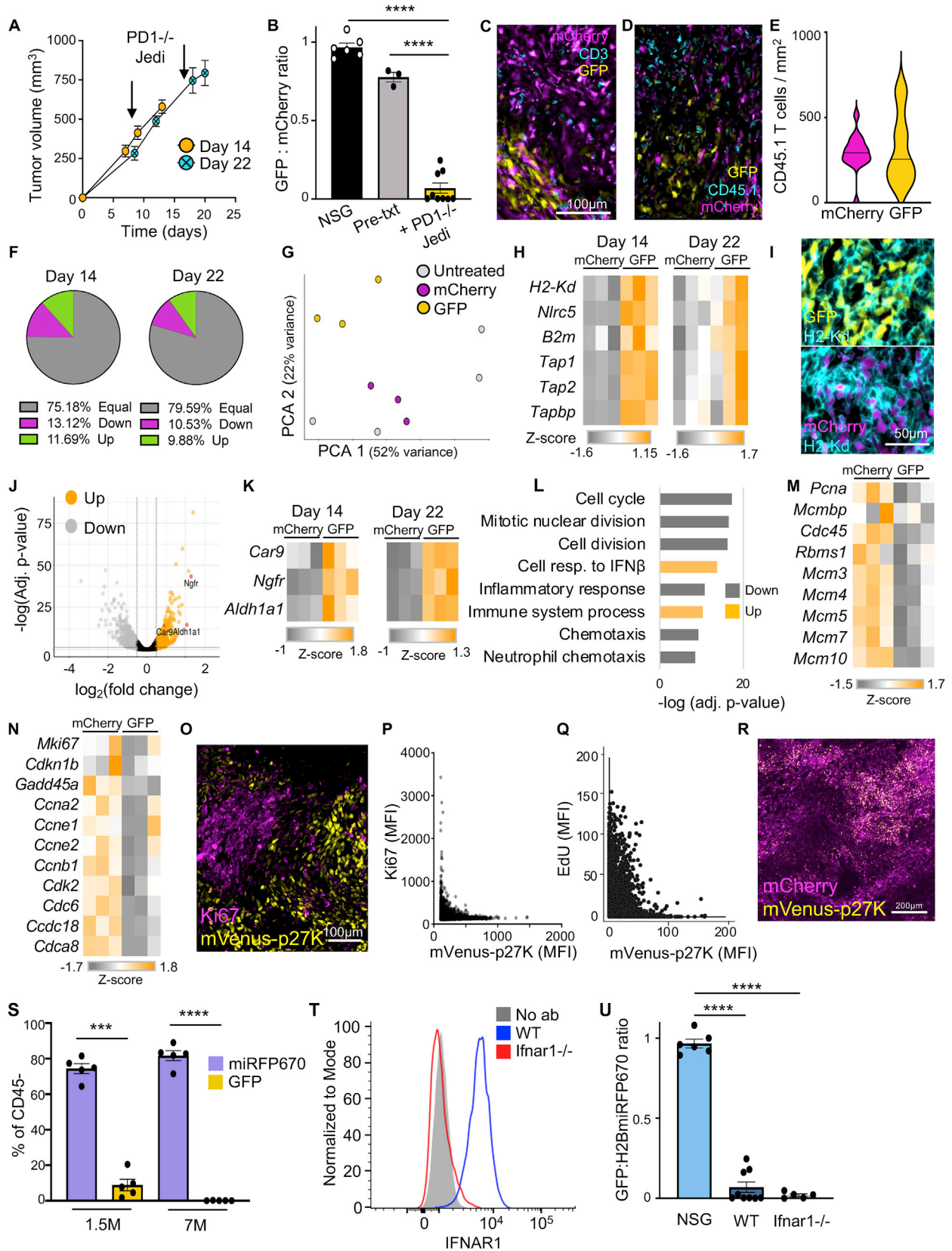


Figure S1. Breast tumor cells that escape from PD1^{-/-} T cell killing express MHC1 and the antigen presentation genes and are quiescent

- (A) Graph shows tumor volume over time from mice in Figure 1A. The mean \pm SEM of the volume is shown. Arrow marks time of T cell injection.
- (B) Quantification of GFP⁺ cells killing by Jedi T cells. GFP⁺ and mCherry⁺ 4T07 cells were mixed at 1:1 ratio and injected in the mammary fat pad of either NSG or BALB/c mice. 7M of PD1^{-/-} Jedi T cells were adoptively transferred at day 7. Graph shows GFP/mCherry ratio (mean \pm SEM). (n = 3–6 mice).
- (C) Representative immunofluorescence images showing CD3 staining in tumors from mice in (A) at day 22 (n = 3 mice).
- (D) Immunofluorescence analysis of CD45.1⁺ PD1^{-/-} Jedi T cells inside tumors of mice in (A) at day 14. Representative image is shown (n = 3 mice).
- (E) Number of T cells per tumor area from images in (D). Graph presents the density of CD45.1⁺ cells in either GFP⁺ or mCherry⁺ regions. Bar marks the median (Multiple areas from 3 tumors).
- (F) RNA-sequencing was performed in mCherry⁺ versus GFP⁺ cancer cells from tumors in Figure 1A. Pie charts show the percentage of statistically differentially expressed genes.
- (G) Principal component analysis (PCA) of RNA-seq data from mCherry⁺ and GFP⁺ tumor cells in mice from (A) from day 22, and from mCherry⁺ tumors from untreated mice (n = 3–4 mice).
- (H) Heatmap shows key genes in the antigen presentation machinery from mice in Figure 1A. Data is color coded to reflect gene expression Z scores.
- (I) Immunofluorescence images of H2-Kd (MHC1) in tumors from mice in (A). Representative images are shown (n = 3 mice).
- (J) Volcano plot showing log₂ fold-change differences versus $-\log(\text{adjusted } p \text{ value})$ of GFP⁺ versus mCherry⁺ cells from Figure 1A.
- (K) Heatmap shows differentially expressed genes related to resistance to therapy, tumor initiation, and hypoxia from samples in Figure 1A. Data are color coded to show gene expression Z scores.
- (L) Pathway enrichment analysis from differentially expressed genes in GFP⁺ versus mCherry⁺ cancer cells from RNA-seq from Figure 1A at day 22 (n = 3 mice). Graph shows pathways ranked by lowest adjusted p value.
- (M and N) Heatmaps show key differentially expressed genes in GFP⁺ versus mCherry⁺ cells involved in regulation of DNA replication (M) and cell cycle (N) from Figure 1A. Data are color coded to show gene expression Z scores.
- (O and P) mVenus-p27K reporter in untreated 4T07 mammary carcinoma. (O) Immunofluorescence analysis of Ki67 and mVenus-p27K. (P) Graph depicts the intensity of the fluorescence signal for each marker in each cell.
- (Q) Graph depicts the intensity of the fluorescence signal for each marker in each cell from Figure 1L.
- (R) Double transduced mCherry and mVenus-p27K-expressing 4T07 cells were injected in the mammary fat pad of NSG mice. Image shows a representative area of tumors at day 10 (n = 3 mice).
- (S) Flow cytometry analysis of GFP⁺ and H2B-miRFP670⁺ live tumor cells from mice in Figure 1M. Graph shows mean \pm SEM of the percentage of total live per color among DAPI⁻ CD45⁻ cells per tumor (n = 5 mice).
- (T) Confirmation of loss of IFNAR1 protein in *Ifnar1*^{-/-} cells (in Figure 1Q) by flow cytometry analysis.
- (U) Graph shows quantification (mean \pm SEM) of the GFP/H2B-miRFP670 ratio in the tumors from Figure 1Q.
- ***p < 0.001, ****p < 0.0001.

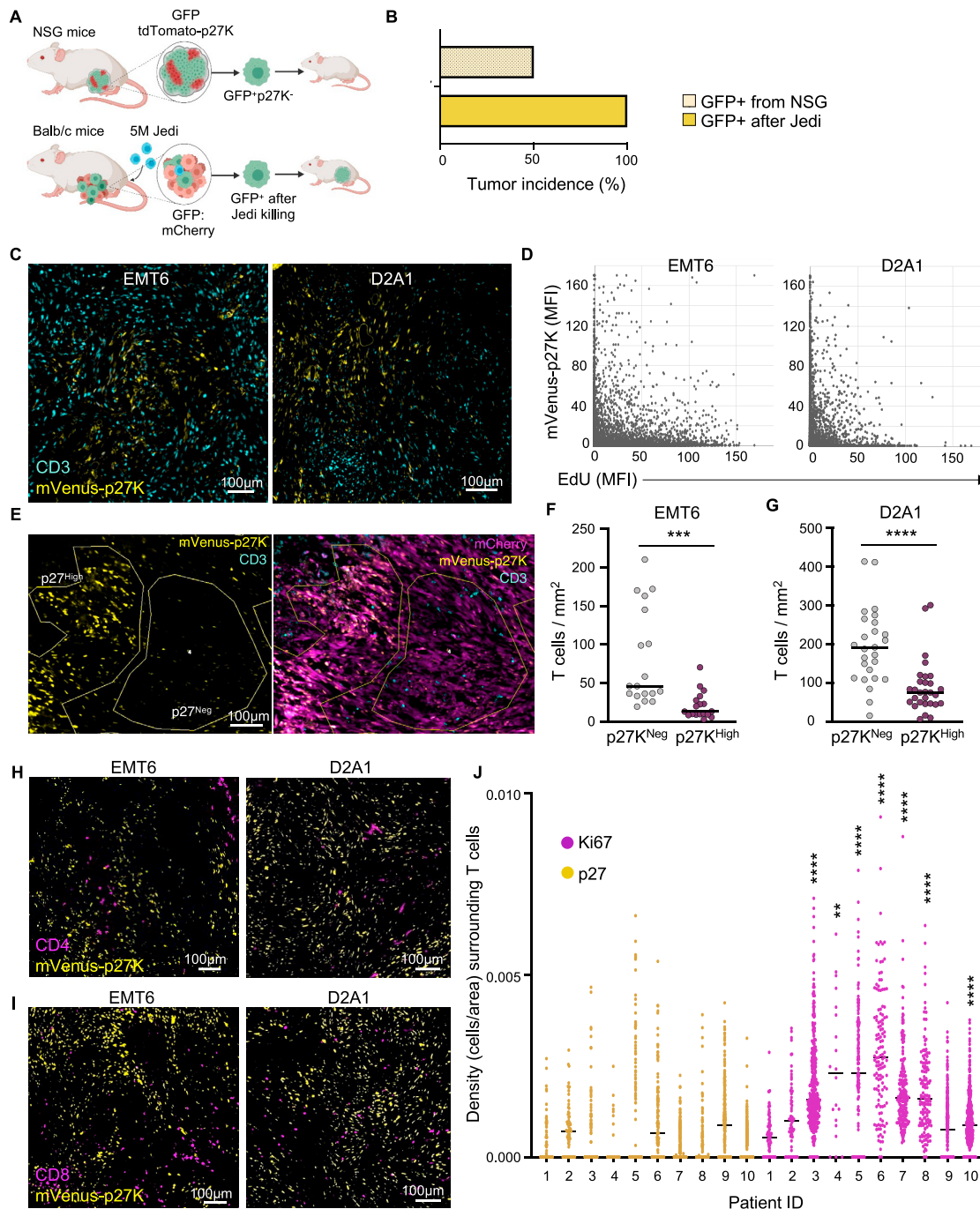


Figure S2. Quiescent breast cancer cells cluster together and exclude T cells

(A and B) Assessment of tumor initiation potential in GFP+ cancer cells that survive T cell attack. GFP+ cells were isolated from 4T07 mammary carcinoma of either untreated NSG mice or from Jedi-treated BALB/c mice. 500 live sorted cells were injected in new mice. (A) Schematic of experiment. (B) Percentage of tumor growth (n = 4).

(C and D) Mice with mVenus-p27K-expressing EMT6 or D2A1 carcinoma were treated with EdU for the last 5 days prior harvesting tumors.

(E) Immunofluorescence analysis. (D) Graph depicts the intensity of the fluorescence signal for each marker in (E) in each cell.

(F and G) Quantification of T cell density in mVenus-p27K^{High} versus mVenus-p27K^{Neg} areas in (F) EMT6 and (G) D2A1 tumors. Bars mark the median. (n = 20 images from 3 mice).

(H and I) Representative image of the regions of interest analyzed for Figure 2E (n = 28 images from 3 mice).

(legend continued on next page)

(H and I) Representative images from immunofluorescence of CD4 (H) and CD8 (I) in mVenusp27K-expressing tumors (n = 3 mice).

(J) Analysis of density of p27+ and Ki67+ cells surrounding T cells (CD3) infiltrating tumor bed (E-cadherin) per patient. Each dot represents the density of p27+ or Ki67+ tumor cells in the area surrounding a tumor infiltrating T cells. Statistical significance was assessed between p27+ and ki67+ cell densities in each patient. Bars mark the median. **p < 0.01, ***p < 0.001, ****p < 0.0001.

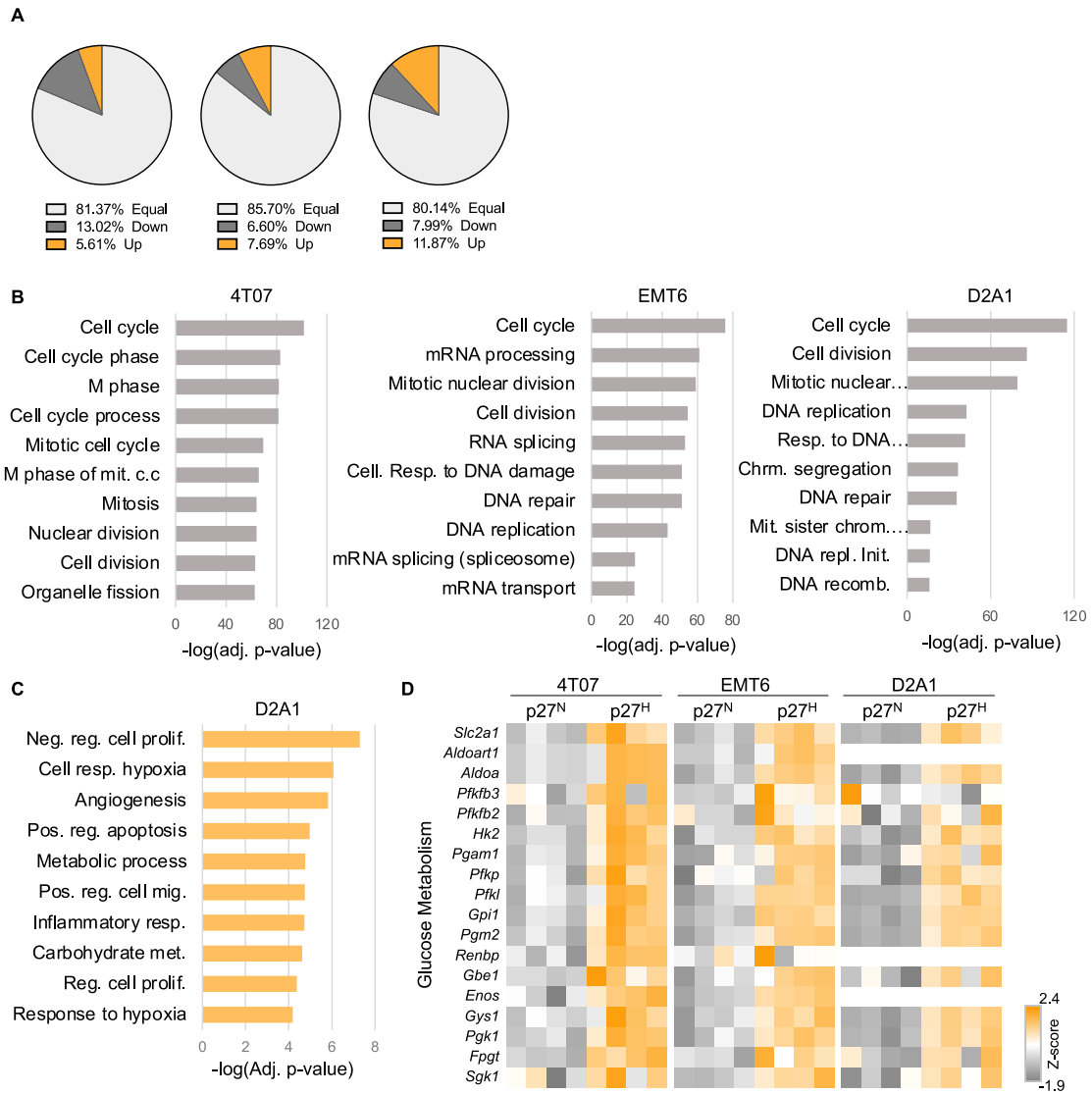


Figure S3. p27^{High} breast cancer cells show signatures of quiescence, glycolysis, and hypoxia

(A) Pie charts show the percentage of differentially expressed genes in cells from Figure 3A (4T07, n = 4; EMT6 and D2A1, n = 3, respectively).

(B) Pathway enrichment analysis of RNA-seq from Figure 3A showing top downregulated pathways ranked by adjusted p value.

(C) Pathway enrichment analysis from D2A1 tumors in Figure 3A showing top upregulated pathways ranked by adjusted p value.

(D) Heatmaps show key differentially expressed genes in RNA-seq from Figure 3A that are involved in glycolysis from GO terms shown in Figures 3B and S3C. Data is color coded to reflect gene expression Z scores.

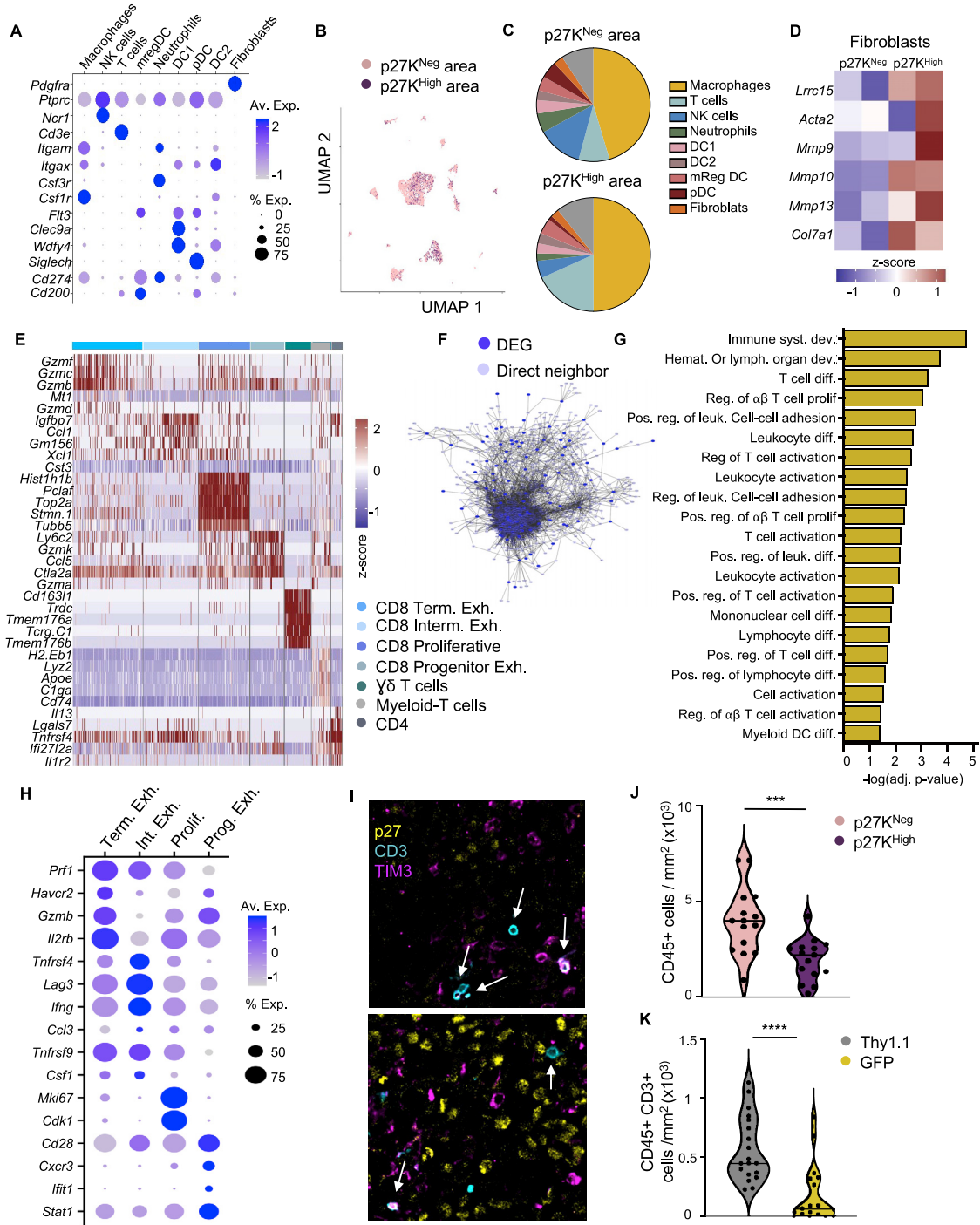


Figure S4. Single-cell RNA-seq analysis showed more exhausted T cells inside tdTomato-p27K^{High} regions

(A) Expression of key genes used for identification of major populations.

(B and C) Infiltrate distribution in the p27K^{High} and p27K^{Neg} areas. (B) Color coded UMAP from Figure 4C to visualize infiltrates in each area. (C) Pie charts show the cell composition in each type of tumor niche.

(D) Heatmap shows key differentially expressed genes in fibroblasts inside p27K^{High} regions compared with p27K^{Neg} areas. Depicted genes were identified in Dominguez et al. (2020). Data are color coded to reflect gene expression Z scores.

(E) Heatmap shows key differentially expressed genes among T cell populations identified in Figure 4F. Data are color coded to reflect gene expression Z scores.

(F) Co-expression gene network in CD8+ T cells visualized by Cytoscape (ver 3.7.1). The largest connected-component with only the DEGs and their direct neighbors are shown here.

(legend continued on next page)

(G) Pathway enrichment analysis from direct neighbors only. Graph shows only the T cell related-pathways ranked by lowest adjusted p value.

(H) Expression of key genes used for identification of CD8 T cell populations from [Beltra et al. \(2020\)](#) and [Miller et al. \(2019\)](#).

(I) Representative pictures from [Figures 4J](#) and [4K](#). Arrows point to T cells.

(J) Quantification of CD45+ cell density in the different tumor areas from [Figures 4J](#) and [4K](#). Bar marks the median (Multiple regions were quantified from 4 different tumors).

(K) Quantification of CD3+ cells density in the different tumor areas from [Figures 4L–4N](#). Bar marks the median (Multiple regions were quantified from 3 different tumors). ***p < 0.001, ****p < 0.0001.

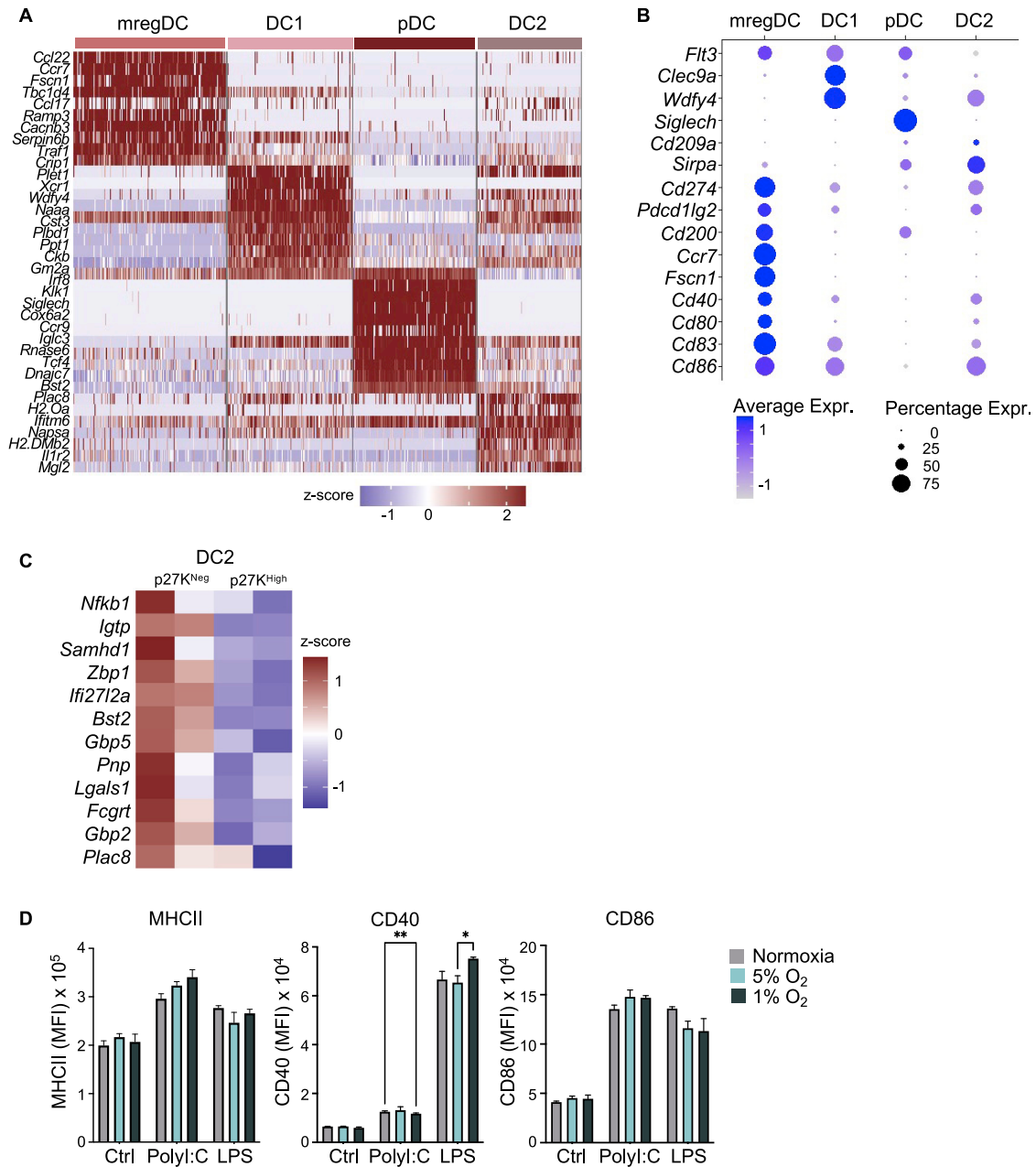


Figure S5. Dendritic cells show lower expression of genes involved in T cell activation and higher levels of pro-tumor genes

(A) Heatmap of key differentially expressed genes in DC subsets from Figure 4C. Z score normalized data is shown.

(B) Dot-plot of key genes used for identification of the specific dendritic cell (DC) subsets.

(C) Heatmap of averaged differential expression of relevant genes in Figure 5B across DC subsets.

(D) Bone marrow-derived DCs were treated with LPS or PolyI:C for 18 h while exposed to different oxygen levels. DCs were pre-conditioned at the specified oxygen concentration for 2 h prior to adjuvant treatment. Graph shows mean ± SEM of MFI for depicted activation markers (n = 3).

*p < 0.05, **p < 0.01.

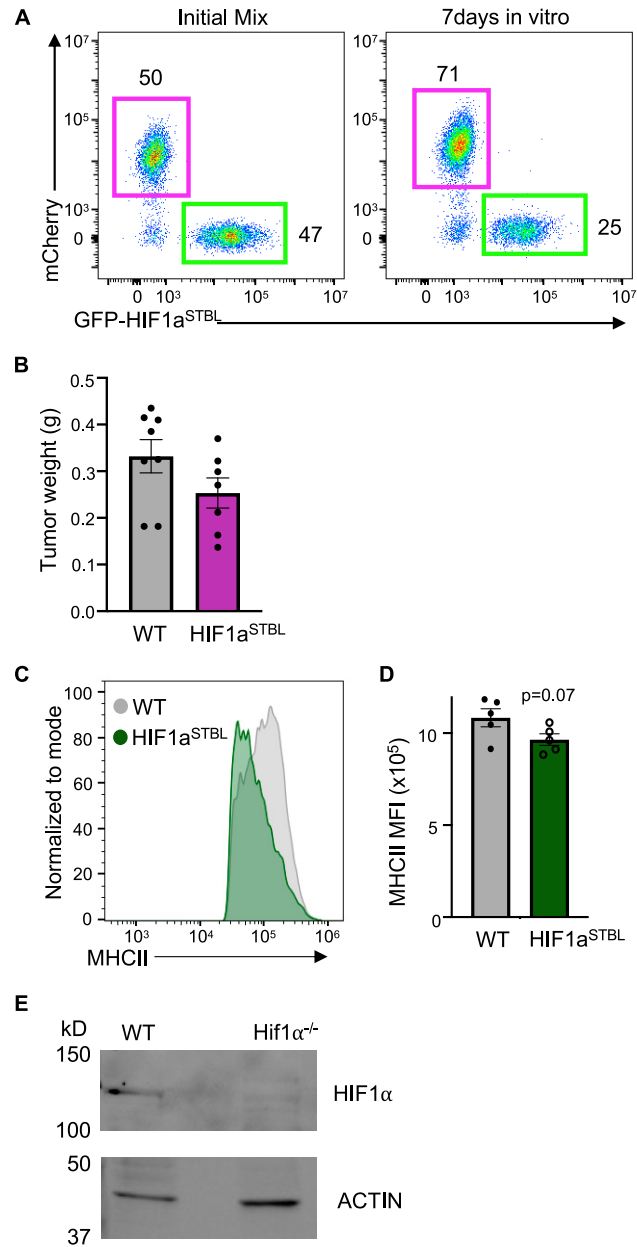


Figure S6. HIF1a activation in tumor cells leads to less activated DCs and exhausted T cells

(A) WT mCherry+ 4T07 cells were seeded 1:1 ratio with HIF1a^{STBL} GFP+ 4T07 cells and cultured for 1 week. Representative flow cytometry plots are shown.

(B) Tumor volume from Figure 6A.

(C and D) MHCII staining in tumors from Figure 6F. (C) Representative histogram. (D) Graphical representation of mean ± SEM of MFI.

(E) HIF1A levels in WT and Hif1a^{-/-} 4T07 cell lines by western blot.